JOURNAL OF GEOPHYSICAL RESEARCH, VOL. 112, E10001, doi:10.1029/2006JE002886, 2007

Solar energetic particles in near-Mars space

J. G. Luhmann,[1] C. Zeitlin,[2] R. Turner,[3] D. A. Brain,[1] G. Delory,[1] J. G. Lyon,[4] and W. Boynton[5]

Received 21 December 2006; revised 22 February 2007; accepted 9 August 2007; published 2 October 2007.

[1] The space radiation environment near Mars has taken on new interest due to the resurrection of plans to send humans to explore the red planet. In addition, solar energetic particles represent a possibly significant input of energy to the atmosphere of Mars during major events, with consequences for atmospheric ionization, chemistry, and possibly escape. Measurements of solar events by the MARIE and GRS experiments on Mars Odyssey illustrate how Mars affects the low-Mars-orbit fluxes of these particles, apparently blocking some particles' access to the spacecraft. The extent to which the presence of Mars reduces the fluxes in Mars orbit from their interplanetary values, and the circumstances and geometry of those reductions, is examined using a simple model and some observationally inspired assumptions about the nature of solar energetic particle events. The results suggest how Mars orbiter SEP results can be interpreted, and also how near-Mars fluxes for a particular interplanetary event can be predicted.

Citation: Luhmann, J. G., C. Zeitlin, R. Turner, D. A. Brain, G. Delory, J. G. Lyon, and W. Boynton (2007), Solar energetic particles in near-Mars space, *J. Geophys. Res.*, *112*, E10001, doi:10.1029/2006JE002886.

1. Introduction

[2] The MARIE investigation on Mars Odyssey [*Zeitlin et al.*, 2004] is the second energetic particle detector placed into orbit around a terrestrial planet other than Earth. The SLED instrument on Phobos-2 [*McKenna-Lawlor et al.*, 1992, 2005], its predecessor, made measurements in a highly elliptical initial orbit, before settling into a near-circular ~2.78 Mars radius orbit near the orbit of Phobos, its primary target body. In contrast, Odyssey was placed in a high-inclination Mars mapping orbit at ~400 km near the terminator plane, with a period of approximately two hours. The purpose of the MARIE investigation was to monitor the potential space radiation hazards at Mars, specifically from energetic ions, in anticipation of eventual human exploration. From earlier missions, and most directly from Mars Global Surveyor (MGS) magnetic field measurements [*Acuña et al.*, 1999], it is known that Mars possesses no significant global dynamo field capable of either shielding Mars from solar energetic ion influxes, or of trapping radiation belt particles. Therefore expectations for modification of the interplanetary fluxes of solar particles by Mars were much different than those for Earth, although *Leblanc et al.* [2002] suggested there might be a localized region around the strongest and largest southern hemisphere crustal fields that experienced some magnetic shielding from incoming ~MeV ions.

[3] The MARIE experiment, designed to identify the charge and energy of ~20-200 MeV ions of either solar or galactic origin, measured a significant number of apparently solar space radiation increases during its 20 month period of operation [*Cleghorn et al.*, 2004]. Two instruments of the Gamma-Ray Spectrometer (GRS) instrument suite [*Boynton et al.*, 2004], the Gamma Sensor (GS) and the High-Energy Neutron Detector (HEND) aboard Odyssey, are also sensitive to energetic charged particles, though their primary purpose is to search for hydrogen and, in the case of the GRS, to create elemental maps of Mars. (The GS's Upper Level Discriminator, or ULD, efficiently records charged particles with an energy threshold of about 35 or 40 MeV for protons. The sensitivity of HEND is more complicated, and will not be discussed further here, but we note that it measures the same periodic oscillations as are seen in the other detectors.) A notable attribute of the Odyssey solar energetic particle (SEP) event measurements is a consistent orbital modulation, also observed on Phobos-2 during its elliptical transfer orbits. Backgrounds in several other detectors, such as the Electron Reflectometer on Mars Global Surveyor, which has a mapping orbit at around the same altitude as Odyssey, also show orbital modulations during solar events [*Brain et al.*, 2006]. The Odyssey instruments typically detect peak rates when passing over the North Pole of Mars and substantially lower rates when passing over the South Pole. While the obvious explanation for these modulations is that Mars is "shadowing" or absorbing some of the solar energetic particles in particular locations, it is of interest to determine both the circumstances of such shadowing, and how it alters the near-Mars radiation environment during solar events compared to the interplanetary radiation environment. Such knowledge can be used for both practical applications in

[1]Space Sciences Laboratory, University of California, Berkeley, Berkeley, California, USA.
[2]Lawrence Berkeley National Laboratory, Berkeley, California, USA.
[3]ANSER, Arlington, Virginia, USA.
[4]Physics and Astronomy Department, Dartmouth University, Hanover, New Hampshire, USA.
[5]Lunar and Planetary Laboratory, University of Arizona, Tucson, Arizona, USA.

0148-0227/07/2006JE002886$09.00

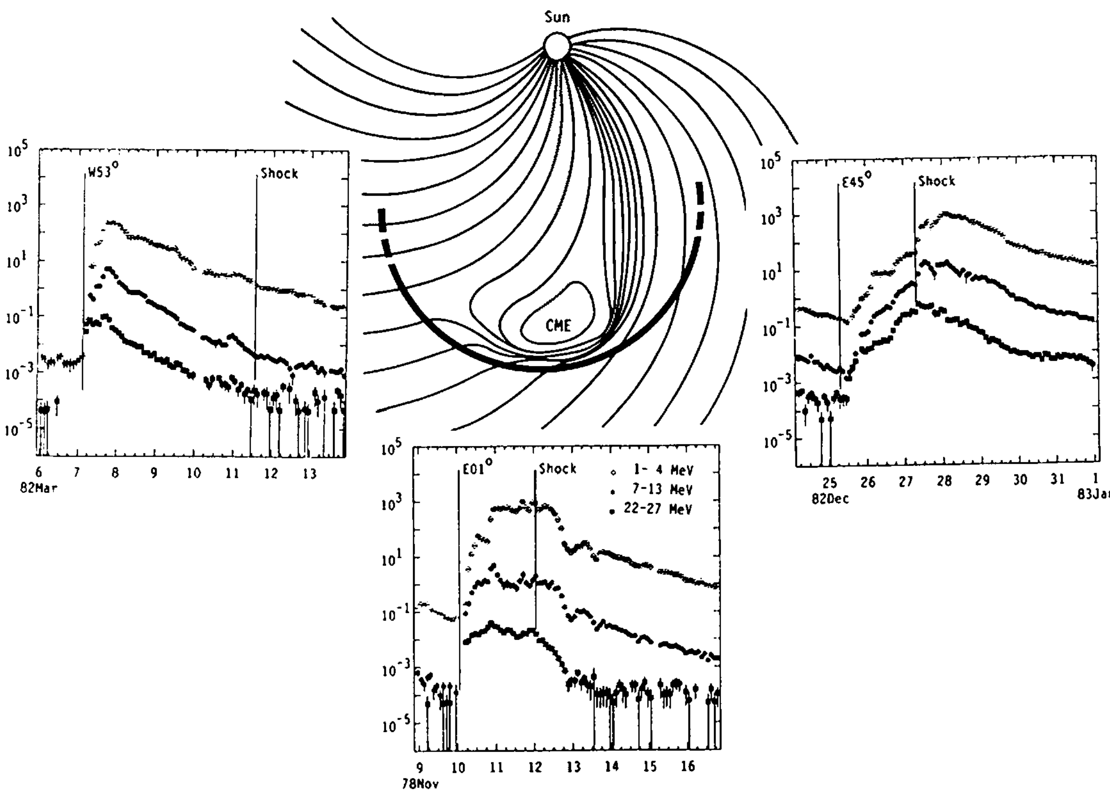

Figure 1. Figure from *Reames* [1999] illustrating the dependence of gradual SEP event time profiles on an observer's location with respect to the solar event that drives the interplanetary shock source. "CME" stands for coronal mass ejection, the typical shock driver. The shock source is strongest at the nose (the leading portion of the shock as it expands outward), so that the highest SEP fluxes are usually seen when the observer is connected by interplanetary field lines (thin solid lines here) to that area of the shock.

radiation hazard planning for Mars missions, as well as in assessing the incident flux pattern and particle energy input to Mars' atmosphere and surface by SEPs.

[4] Solar energetic ions are predominantly protons, reflecting the composition of the Sun. The SEP ion events detected near the Earth appear to arise from a moving coronal and/or interplanetary shock source accelerating particles out of the ambient medium, and from solar flare site-accelerated particles [e.g., *Kallenrode*, 1996; *Reames*, 1999]. The largest events are the so-called gradual events, which can last up to several days and have been associated with fast coronal mass ejection-driven shocks. These typically exhibit a rapid rise in proton fluxes on a timescale of tens of minutes to an hour, sometimes followed by a second, occasionally higher intensity peak at energies <50 MeV when the interplanetary shock arrives at the observer. The details of the profile also depend on where the observer is located relative to the moving shock source. For example, sometimes the prompt particles do not show a separate peak, and sometimes there is only a prompt peak. Figure 1 illustrates the now widely accepted paradigm for gradual SEP proton event time profiles based on a statistical study by *Cane et al.* [1988] that has since been confirmed by several multipoint-spacecraft studies. This concept is based on the idea that solar energetic protons tend to move along interplanetary magnetic field lines from their sources. If their source is a shock front that is strongest at its nose, the highest fluxes are seen when the interplanetary magnetic flux tube through the observer intersects the shock closest to that area. The enhancement when the shock arrives, also referred to as an ESP or Energetic Storm Particles peak, is due to detection of particles accelerated at the shock that are not (yet) energetic enough to have escaped their source region.

[5] Figure 2 shows two examples of SEP time profiles obtained with MARIE and GRS on Odyssey. The vertical gridlines in both plots correspond to times when Odyssey was almost directly over the North Pole of Mars. The event on 28–29 October 2002, shown in Figure 2a, appears to have a single peak that takes a large fraction of a day to reach its maximum, suggesting the prompt peak was not detected in this case. In contrast, the event on 18–20 March 2003, depicted in Figure 2b, shows a classic sudden increase, and later a second increase. The gap in the MARIE time series is due to its inability to acquire new data while old data were being downloaded; the GRS data provide continuity, albeit with a higher energy threshold. Below each time profile the planetary latitude and longitude of Odyssey are shown for reference. Note that the strongest crustal magnetic fields are located in the southern hemisphere near 180 degrees longitude. In general, the SEP event profiles observed by MARIE are as expected from the near-Earth SEP observations. This was also noted in comparisons of MARIE SEP with events detected at Earth on

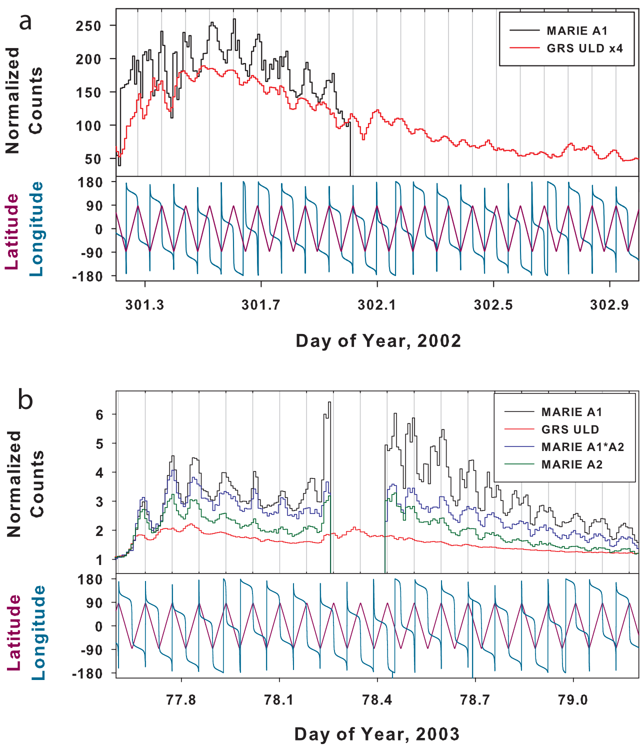

Figure 2. (a) The SEP event of 28 October 2002. At top, the MARIE A1 and GRS count rates relative to 2002 solar quiet time (the GRS rate has been multiplied by 4 for better visibility). At bottom, Odyssey's latitude and longitude during the event. (b) The less intense SEP event of 18-20 March 2003, showing (top) data from the MARIE A1 and A2 counters, the MARIE coincidence trigger, and the GRS ULD, along with (bottom) Odyssey's latitude and longitude.

the GOES spacecraft [e.g., *Zeitlin et al.*, 2004]. However, the distinctive oscillations of ~ two hour duration (equal to the orbit period, which is actually 118 min and 35 s) are unique to Odyssey's low Mars orbit environment. Here we will consider the origin and nature of these oscillations, and what they tell us.

[6] Before considering the SEP oscillations in more detail, it is important to note that the Odyssey orbit is not perfectly circular. It reaches periapsis, at an altitude of 390 ± 5 km, when the spacecraft is near the South Pole, and apoapsis, at an altitude 454 ± 5 km, near the North Pole. (The longitude of periapsis oscillates within ±9° of 270°, so it does not occur precisely over the South Pole.) For an isotropic influx of particles, this has the effect of introducing a varying Mars shadowing effect into the count rates for the GRS ULD and the MARIE counters that has the same phase as that seen during some SEP events. However, in Odyssey's case it is a very small effect, with a peak-to-valley difference of about 2% of the count rate. In the SEP events, the peak-to-valley differences vary but are typically on the order of 20 to 40%. Thus the orbital altitude variations cannot account for the observed SEP oscillations.

[7] In the analysis below, we make use of both types of MARIE data. The two types are coincidence and counter, with the coincidence data have a 30 MeV threshold and a FOV restriction of about 75° (i.e., the viewing cone has a half-angle of about 38°). The A1 counter has a 20 MeV threshold and, in the forward hemisphere, has a field of view restricted only by Mars. The rear FOV is restricted by Mars and also shielded by various spacecraft components. The A2 counter is similar, but with a 30 MeV proton energy threshold. The shielding behind MARIE stops particles with energies below about 175 MeV, so that the measured SEPs all come from the forward hemisphere. The SEP oscillations are always seen most clearly in the MARIE A1 counter data.

[8] The GRS ULD data, like the MARIE counter data, have no angular restriction except that imposed by the shadow of Mars. From Odyssey's orbit, Mars subtends about 27% of the 4π solid angle on average, in a cone of half-angle 63°. In the following, when we refer to FOV restrictions, they can be either those imposed by the shadow of Mars, or, in the case of MARIE coincidence data, the tighter restriction imposed by the experimental trigger geometry.

2. SEPs Near Mars

[9] *Turner et al.* [2003] considered the phasing of the SEP event oscillations in the March 2003 event, and in particular the association between the phase and planetary latitude. If there were some planetary remanent field control, one would expect to observe a consistent phase throughout the event, or until the causative underlying remanent field changes due to the planet's rotation. Figure 3 illustrates the Odyssey orbit. The SEP event time profile for the March 2003 event (Figure 2b) suggested that initially the phase of the oscillations was consistent with a maximum over the North Pole, but then the phase shifts. In the early part of the event, oscillations are seen in all MARIE data (A1 counter, A2 counter, and coincidence) as well as in the GRS ULD data. Around day 78.6, the A1 and coincidence data begin to show two peaks, one of which usually occurs close to the passes over the North Pole, but an earlier one not so aligned. At about the same time, the MARIE A2 and GRS ULD count rates become noticeably smoother, i.e., the oscillations cease. The energy threshold of the A2 counter is the same as that for the coincidence data; the difference is most likely due to the tighter FOV restriction in the coincidence data. The A1 counter, with a significantly lower energy threshold, continues to show oscillations.

[10] A similar degree of complexity is also apparent in the more intense event shown in Figure 2a; MARIE coincidence data are unavailable for this event due to rate limitations of the pulse-height readout. However, the A1 counter data are of interest, showing peaks at every pass over the North Pole. Peak to valley ratios are on the order of 1.3 to 1.4 from about day 301.2 until MARIE stopped recording data. Double peaks are seen in some instances. For day 302, with MARIE off, the GRS data show continuing oscillations into the second day of the event. The last large peak that is well-aligned with a North Pole pass occurs at about day 302.1; subsequent peaks come with a frequency shorter than the orbital period, and then disappear from about 302.5 to 302.8, at which time the flux increases and the alignment is briefly restored. (The ULD data for days 303–305 are generally smooth and without significant peaks; MARIE turned back on at day 304.0 and recorded

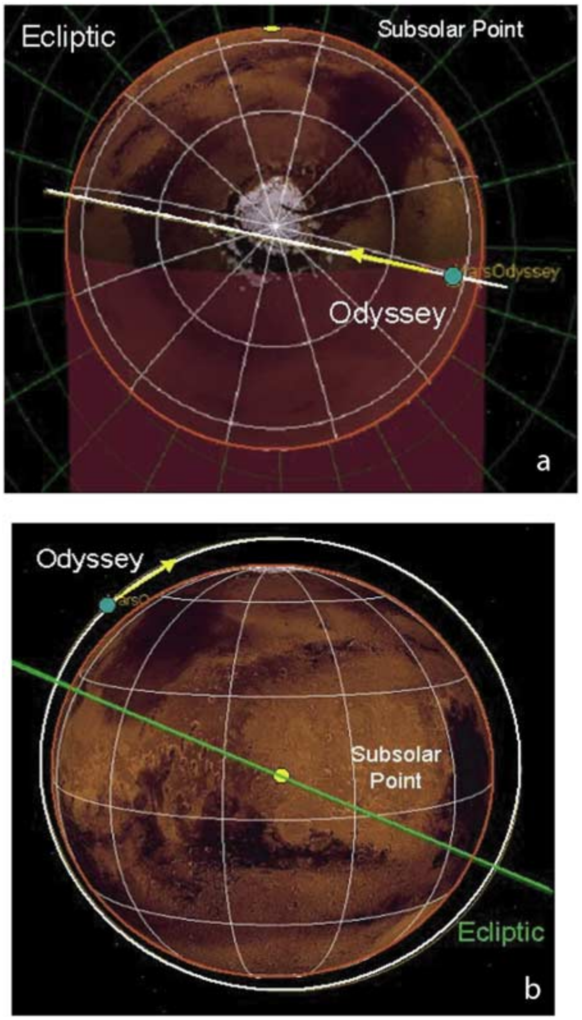

Figure 3. (a) Projection of Mars and the Odyssey orbit, looking down on the North Pole. (b) Mars and the Odyssey orbit as seen from the Sun.

more peaks over the course of day 304, though none are aligned with North Pole passes. The ULD count rate had fallen back to within 25% of its quiet time value by day 305.0.)

[11] To understand the general behavior of MeV SEP protons in the space around Mars, we first consider the local interplanetary magnetic field (IMF) perturbation due to the solar wind interaction, and whether it can have a significant effect on such energetic particles. The particles most sensitive to a particular magnetic field structure will be those that stream approximately parallel to the magnetic field in interplanetary space. In fact the prompt portion of the SEP event is often found to be quite anisotropic, probably due to the fact that the particles are coming from the shock source when it is still in the corona close to the Sun. The diverging heliospheric magnetic field can cause an isotropic particle distribution arising from a coronal shock to become increasingly focused as the particles stream outward. This is attributable to the mirror force on the particles first in the corona and then in interplanetary space. Thus the protons in the early portion of a SEP event are roughly field-aligned when the observer is magnetically well-connected to the (then) near-Sun source. The draped magnetic fields caused by the Mars solar wind interaction are the next structure they encounter. Their approximate geometry, based on an MHD numerical model of the solar wind interaction with a conducting sphere (see *Kallio et al.* [1998] for details about this model), is illustrated in Figure 4.

[12] It is important to consider the gyroradii of MeV protons in magnetic fields the strength of those around Mars, because that establishes the extent to which we expect to see any effect. For a typical local interplanetary field of about 3 nT, a 1 MeV proton has a roughly 10 Mars radii gyroradius. Even in the strongest (subsolar) region of the draped distorted field (~40 nT), the gyroradius is still about a Mars radius. This means that a field perturbation the size of the Mars solar wind interaction is unlikely to have much effect on the particles' motion. It is too small both in scale and magnitude to matter much. This is borne out by test particle calculations in the magnetic fields shown in Figure 4. The colored, dotted lines in this figure represent 1 MeV proton trajectories approaching Mars from the bottom of the simulation space, along the interplanetary field, which is perpendicular to the solar wind flow in this model. The trajectories of the protons were obtained using a standard finite difference numerical solution of the Lorentz force equation of motion. The colors simply distinguish three different groups of trajectories for clarity. Only modest deflections in these initially field-aligned trajectories are caused by the draped interplanetary field structure around Mars. Thus 20–200 MeV SEPs, such as those measured by MARIE, to first order can be considered unaffected by the draped fields of the Mars-solar wind interaction. This makes a more generalized modeling of the SEP shadows much more straightforward.

3. A Simple Model for SEPs Near Mars

[13] We assume that the observed oscillations during the SEP events observed around Mars result from a combination of the interplanetary angular distribution of the SEPs in a particular event, shadowing/absorption by Mars, and instrument field-of-view constraints. To analyze the effects of various interplanetary field orientation and SEP event realizations on what is measured in an orbit like that of Odyssey, we adopt the simplified model of the space in the vicinity of Mars shown in Figure 5. Here it is assumed that the interplanetary magnetic field is unaffected by the planet. This field can be oriented in any direction corresponding to the field upstream of the Mars solar wind interaction region. We then assume the detector is located at 400 km altitude with respect to the surface of the planet, in the near-terminator local time sector similar to the Odyssey spacecraft orbit in Figure 3. Moreover we assume that the detector has a conical aperture analogous to the MARIE field of view, and that the aperture points in the direction approximately opposite to the spacecraft motion along its orbit, also similar to MARIE (there is a 17° offset between the centerline of the MARIE FOV and the spacecraft's anti-velocity vector). The restricted FOV in the calculation simulates the MARIE data obtained with the coincidence trigger.

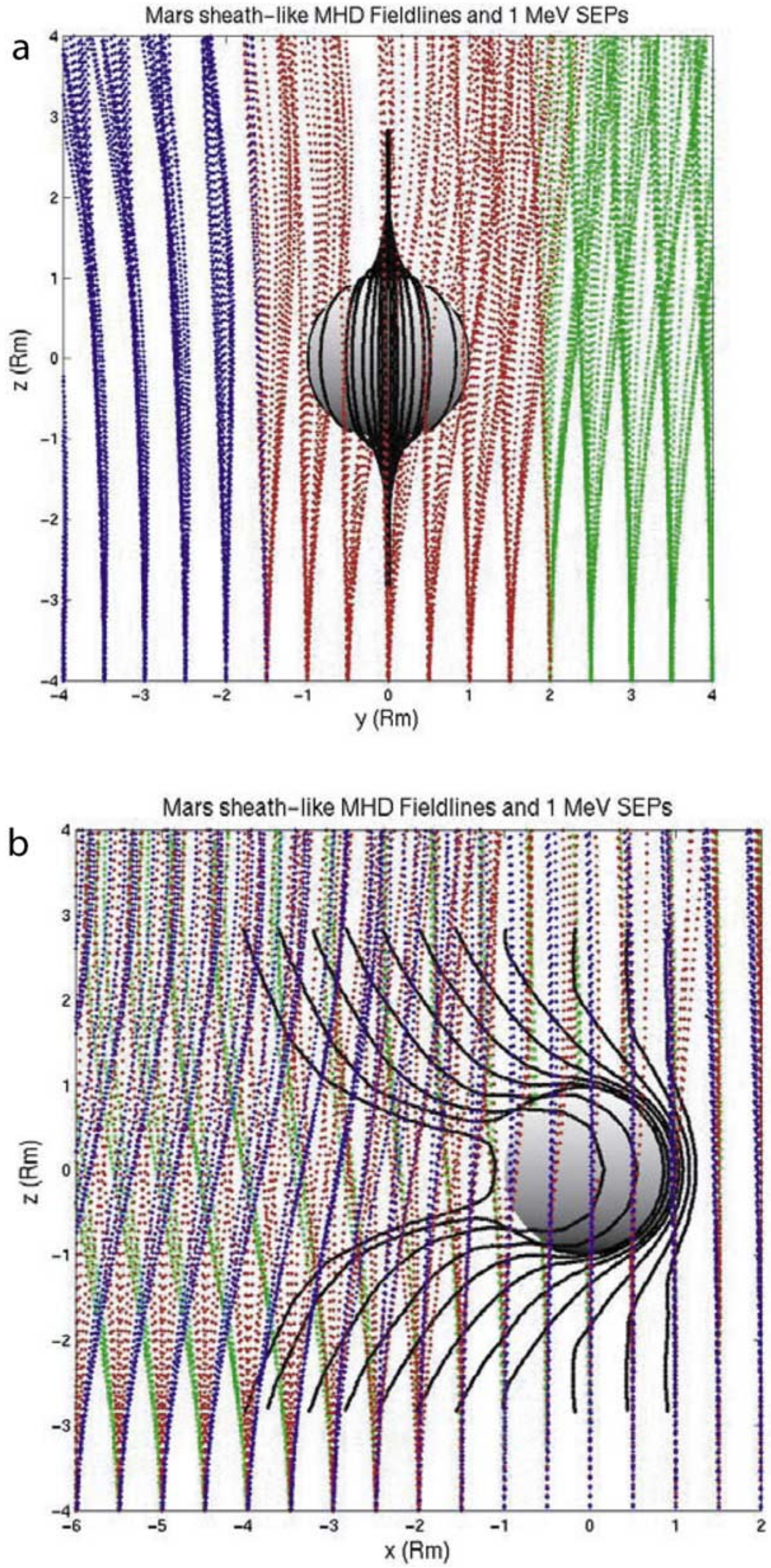

Figure 4. (a) View from the Sun of the innermost draped fields from an MHD simulation of the Mars solar wind interaction (black lines) and projections of the 3-D trajectories of 1 MeV proton test particles launched upward along the field into the simulation space from a grid of starting points at the bottom. (b) View looking down on the plane parallel to the undisturbed interplanetary fields. The three colors of the particle trajectories simply identify those from three different sections of starting points divided along the y coordinate. The modest deflections produced by the draped field are nearly negligible near Mars and are smaller for still higher proton energies or those with larger initial pitch angles.

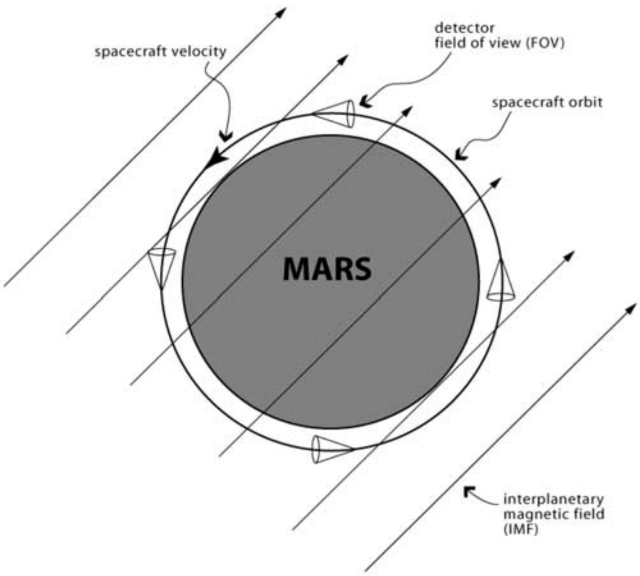

Figure 5. A simplified model of the magnetic fields external to Mars (and its absorbing atmosphere) used in this study of MARIE SEP event oscillations. The orientation of the MARIE conical field of view is also indicated along the illustrated spacecraft orbit.

[14] To investigate which incoming particles are detected at each point in the orbit, we work backward by launching 1 amu test particles of MeV energy from an assumed location of the spacecraft. The strength of the uniform field does not have much of an effect for the range of magnitudes present (∼2–40 nT) near Mars for >1 MeV protons, as the proton trajectories are practically straight lines on the scale of the calculation space shown. Similarly, the proton energy does not matter for the same reason, as those of interest for MARIE are well above the energy where the straight line trajectories are an accurate approximation. Nevertheless, for completeness, we solve the proton equation of motion; this allows future introductions of more complicated field descriptions if desired.

[15] In our calculations 100 particles are followed for a single "injection" from the spacecraft location, which is stepped around the planet 36 steps during each orbital period. Those that intersect the planet (actually the planet plus an assumed spherically symmetric absorbing atmosphere of 200 km altitude) are considered not to have access from space, and are thus considered not detected. Those that reach the outer boundary of the trajectory calculation at 2 Mars radii are considered to have access. The particles can be injected with an isotropic angular distribution, or with an anisotropic distribution beamed along the magnetic field. The latter are approximated by adding an effective streaming velocity parallel to the ambient magnetic field to the injected particle velocities. As the streaming velocity approaches the particle velocity, the particles become increasingly focused along the field direction. Note that there is an interplay between the detector field of view and the particle distribution anisotropy. For example, if the particle distribution is highly beamed, but the magnetic field is oriented at a large angle with respect to the assumed field of view for that point in the spacecraft orbit, no particles may be detected. Similarly, if the beam is along the field, but the field through the spacecraft intersects the planet, no particles will qualify for detected status in our backward tracing scheme.

[16] Some results are shown in Figures 6–8 for a hypothetical SEP event with a time profile exhibiting a prompt peak and then a delayed second maximum. Figure 6 shows the result of the backward tracing of particle trajectories under the assumption that the SEP event is isotropic throughout its duration. The original time profile of proton "flux" or counts as a function of time from the beginning of the event is plotted, and the same event as it is detected at the spacecraft orbit, as the spacecraft circles Mars with an Odyssey-like period. Figure 6a shows the simulated observations without the field of view restriction taken into account. The reduction in the detected intensity, small in this case, is purely due to the shadowing effect of the planet for a detector located at 400 km altitude. Note that a more elliptical orbit with the same periapsis altitude could produce an orbital oscillation with an amplitude equal to the difference between the free space profile and the calculated profile, but as mentioned above this is not a consideration for Odyssey. In Figure 6b a narrow field of view (30 degrees) is introduced with the expected consequence that the observed flux is a significantly smaller fraction of the open-space flux (note the scale is a log flux scale). This field of view restriction, which is slightly more constraining than that of the MARIE coincidence trigger, reduces the modeled "detected" flux to a few tenths of its interplanetary value. (In practice, one attempts to account for this difference by dividing count rate by the appropriate geometry factor, but anisotropy of the incident flux can produce an incorrect result. For example, for MARIE, the geometry factor of the coincidence field of view is 3.19 cm^2 sr, and that of the counter is 20.4 cm^2 sr, in both cases calculated for isotropic incident flux, with the latter number taking account of Mars' shadow.)

[17] Figure 7 illustrates the effect of adding a field-aligned anisotropy to the event, throughout its duration. In this case the anisotropy is created by assuming a streaming velocity of "Vs" (where Vs is 0 to 1 times the particle velocity) that is added to all particle velocities upon injection. The "uniform" interplanetary field (Figure 5) is presumed to lie parallel to the ecliptic, so that the particle flux minima occur when the spacecraft is near the equator in the dawn or dusk sector, depending on the streaming direction of the particles. No field of view restriction, except that due to the shadow of Mars, is imposed in Figure 7a; oscillations are apparent due to the anisotropy. In Figure 7b a significant field of view restriction (60°) is imposed, and it decreases the detected flux by more than an order of magnitude in the minima of the oscillations. Thus the combined effect of anisotropy and the shadow of Mars is sufficient to produce oscillations, but the effect is greatly enhanced by the further restriction of the FOV imposed by a detector telescope's coincidence geometry.

[18] Figure 8 shows the result of imposing a temporally decaying anisotropy, which is more like the situation during a real SEP event. The anisotropy starts with a streaming velocity of 1X the particle velocity and diminishes with a time constant of ∼0.5 day. Detector flux reductions are simulated for the two different fields of view. The oscil-

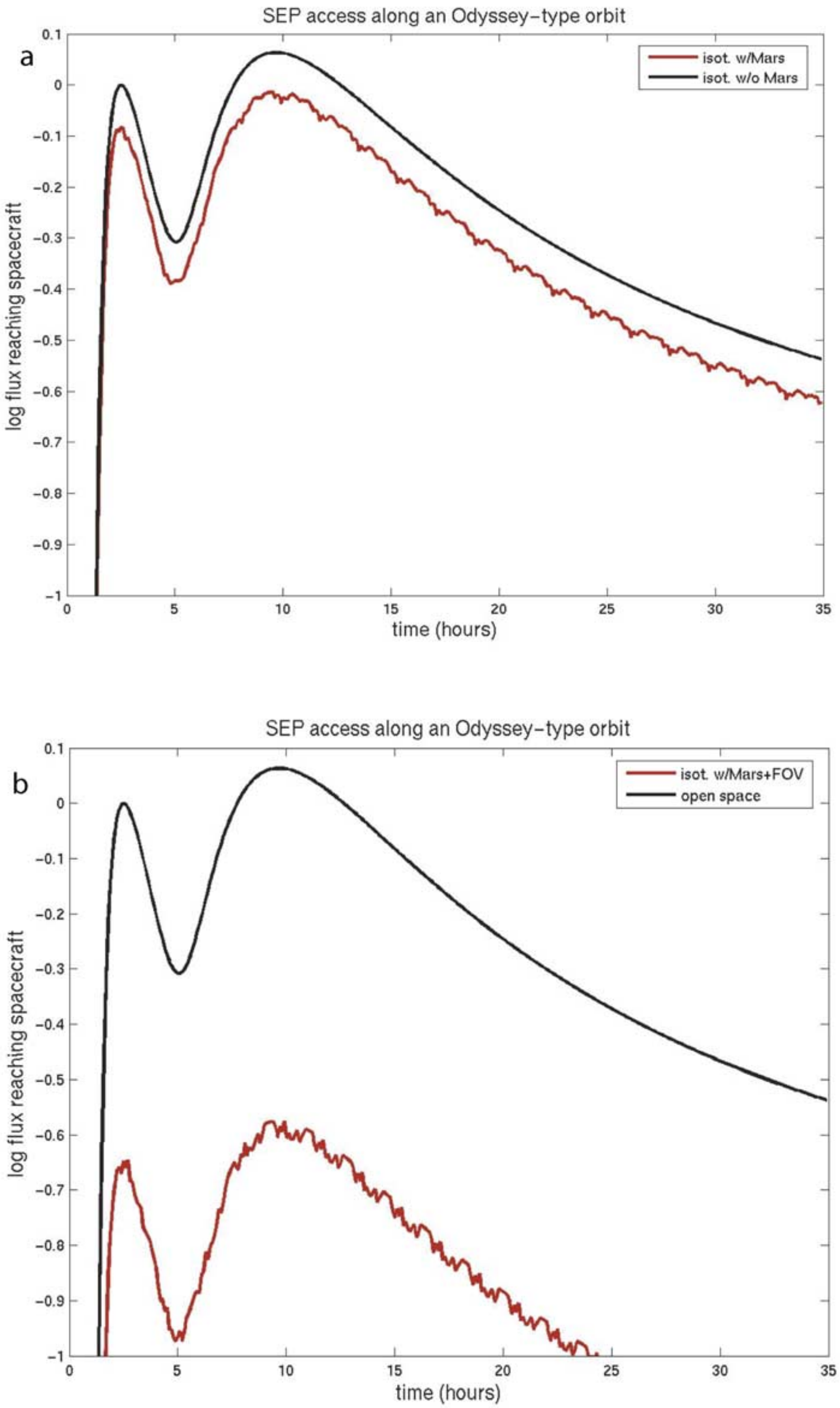

Figure 6. (a) External isotropic event model time series (black) and time series “observed” in an Odyssey-like orbit. Here the reduction in flux is due purely to the shadowing or absorption by Mars, as seen from the 400 km altitude orbit. (b) Same as Figure 6a but with a 30 degree cone-shaped field of view, pointing in the direction shown in Figure 5, imposed on the detection of the particles at the orbit.

lations, which are more pronounced in the narrower (30°) field of view case, die out with the anisotropy as expected. The added effect of a different interplanetary field orientation with the 60° field of view is shown in Figure 9a. In one case the assumed magnetic field is in the ecliptic, with equal components along the Mars-Sun line and in the direction parallel to the orbital motion of Mars, and in the second case the field is pointed north–south in an unusual highly

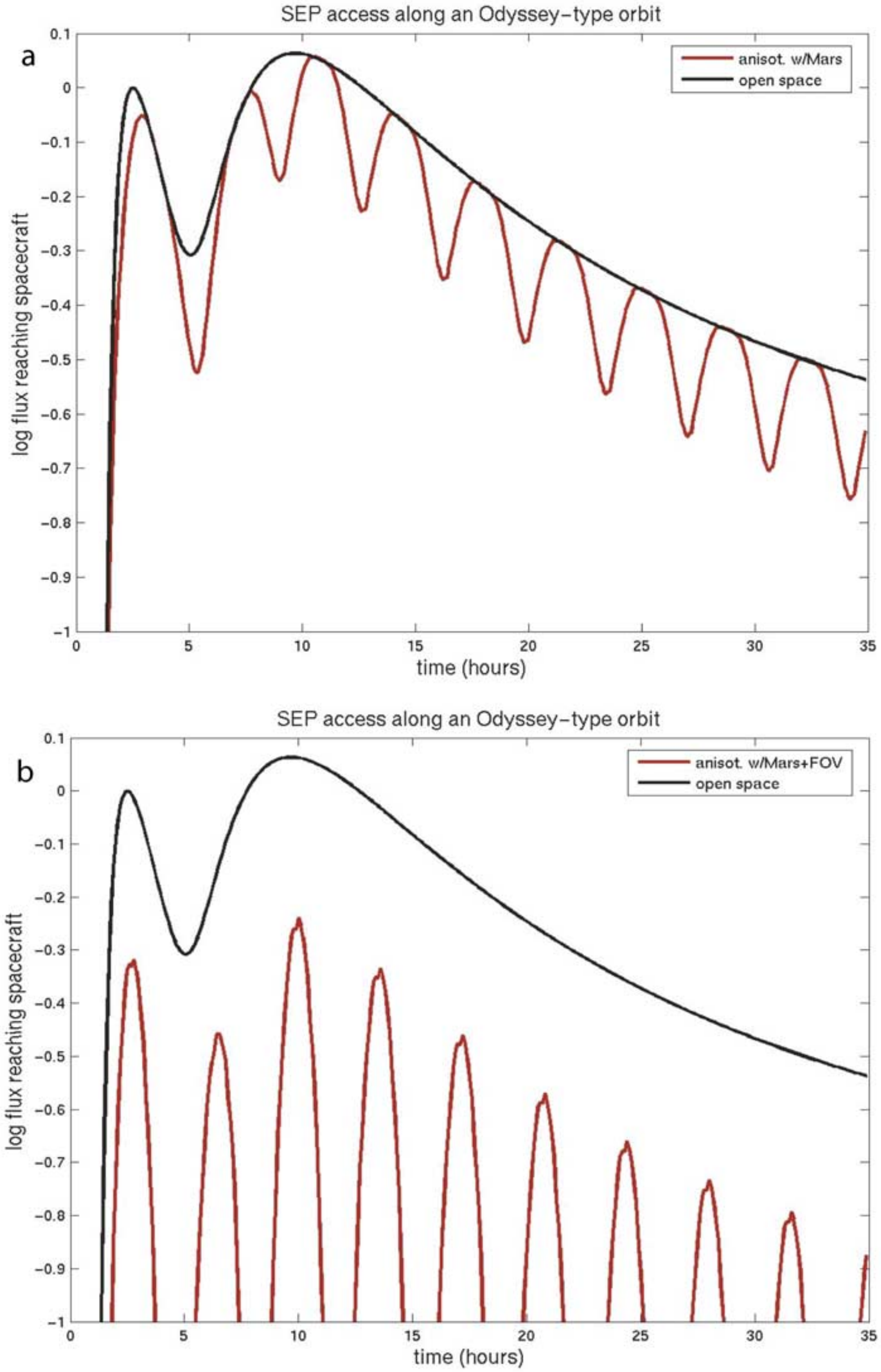

Figure 7. (a) Similar to Figure 6a but with a particle distribution anisotropy created by imposing a field-aligned velocity equal to the particle velocity on the isotropic distributions. (b) Same as Figure 7a but with the field of view restriction added as in Figure 6b.

inclined state, not atypical at the time of large SEP event passages as will be further discussed below. The change of interplanetary field orientation affects the phasing of the detected flux oscillations. When compared against the virtual spacecraft latitude, plotted in Figure 9b, it is seen that the apparent locations of the maxima and minima in the oscillations depend on the interplanetary field orientation, and are not (in this model) connected to any planetary feature. This highlights the ambiguity in interpretation that would occur if the crustal fields of Mars do indeed affect SEP trajectories.

[19] In a sample application of this model, we consider the March 2003 MARIE event in Figure 2b, which is shown in greater detail in Figure 10a, and an interplanetary field orientation inferred from the MGS magnetometer observations over the same period. The interplanetary magnetic

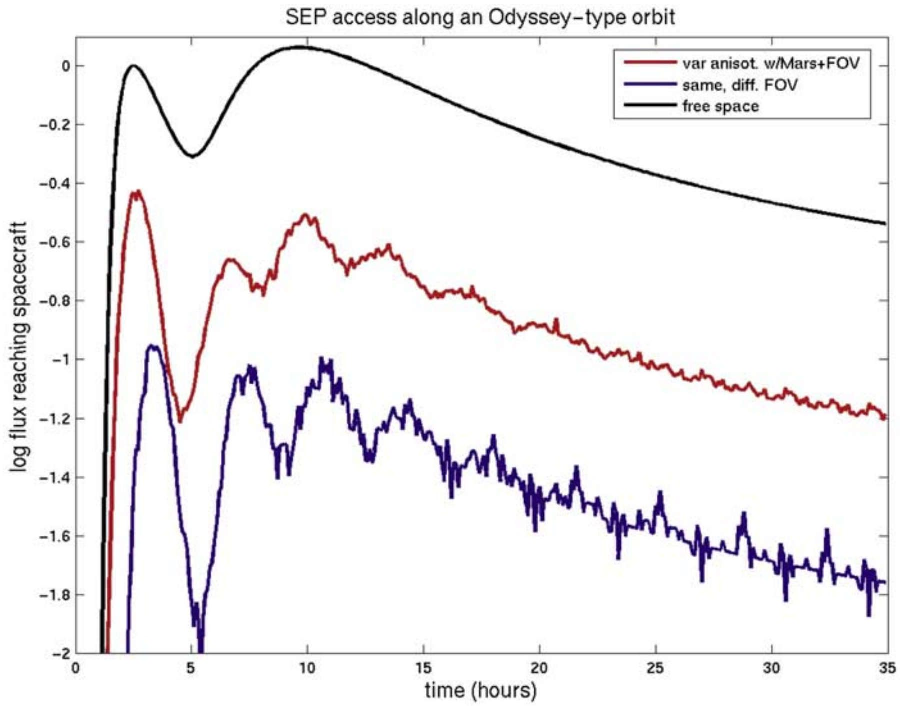

Figure 8. Same as Figure 7 but with an anisotropy that decays on the timescale of a day, and for fields of view with cones of acceptance of 60 degrees (red line, similar to MARIE) and 30 degrees (blue line). The noisiness of the simulated events results from the statistics of the test particle calculation and the impact of factors such as gyrophase.

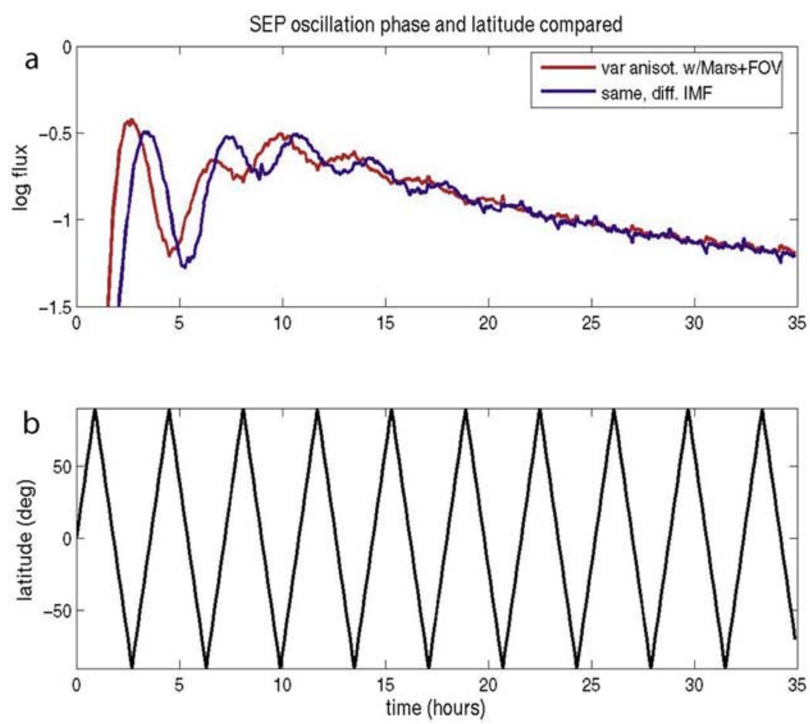

Figure 9. Figure 9a is the same as Figure 8 but for the 60 degree cone of acceptance and two different interplanetary magnetic field orientations, one east–west and one north–south. The interplanetary field orientations determine the phase of the particle flux oscillations with the planetary latitude of the virtual detector (shown in Figure 9b).

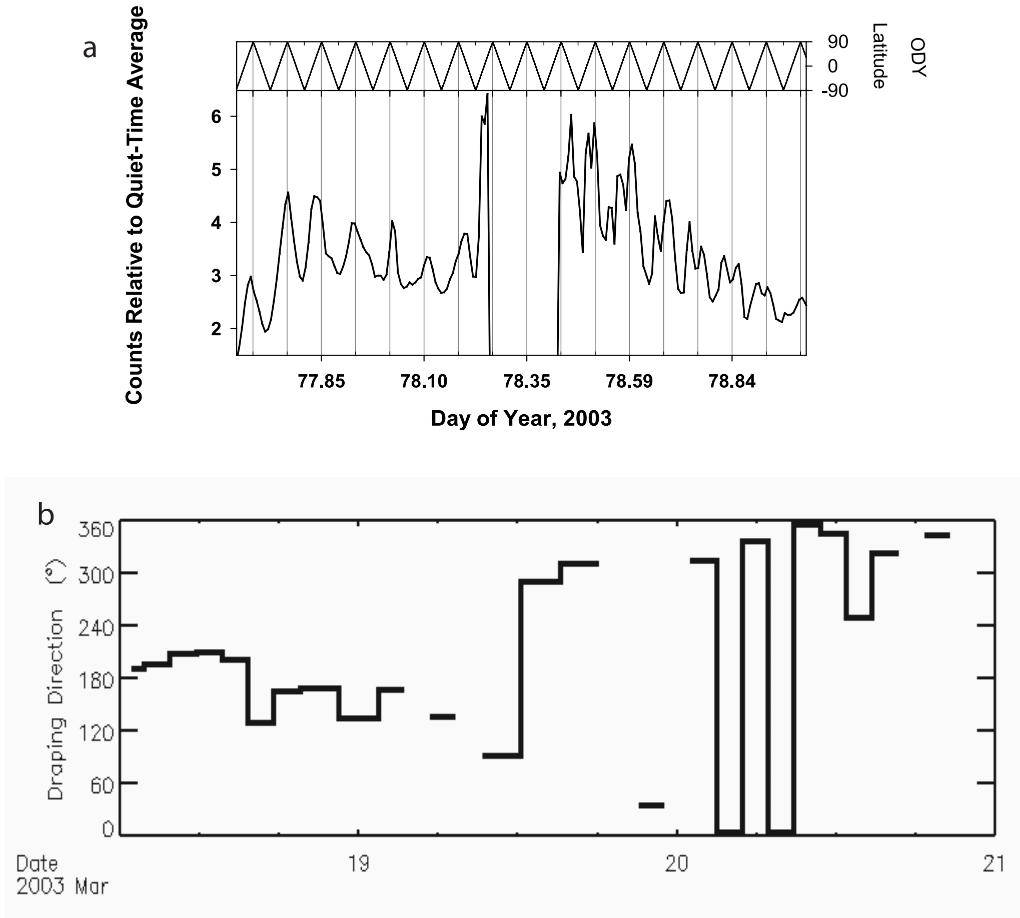

Figure 10. (a) Detailed plot of the March 2003 SEP event observed by the MARIE A1 counter, showing the evolution of the oscillation phase and the appearance of more complex structure in the period from about day 78.5 (midday 19 March) through day 79.0. (b) Plot of interplanetary magnetic field orientation, expressed as angle measured from east, derived from analysis of the MGS dayside magnetometer measurements.

field orientation in the plane perpendicular to the Earth-Mars line, inferred from the orientation of the draped magnetosheath field [see *Brain et al.*, 2006], is shown in Figure 10b. Note that neither the field magnitude nor the Mars-Sun component can be unambiguously obtained from MGS, which orbits Mars at an altitude similar to Odyssey's but in the 2AM-2PM local time plane. However, the abrupt large rotation in the field angle with respect to due east on Mars, in Figure 10b, can be used as a guide and is expected to produce a phase change in the SEP oscillations as discussed above. The results of modeling what an instrument with a 60° field of view in the orientation shown in Figure 5 would detect with the assumed external SEP time profile in Figure 10a and the interplanetary field orientation in Figure 10b is shown by the red profile in Figure 11a. The field orientation in the Mars-Sun direction was obtained via some modest trial-and-error runs. A decaying field-aligned anisotropy in the upstream energetic particle flux through the event is again assumed, but in this case the orbital period of the spacecraft is lengthened to make the oscillation phase change at the time of the interplanetary field rotation more apparent. The qualitative agreement of the simulated event with the observed event reinforces the ideas behind the assumptions made in the present model.

4. Conclusions

[20] Our results suggest several overall conclusions concerning the SEP environment near Mars:

[21] 1. The observed flux of solar energetic particles may be only a small fraction of the interplanetary flux if the flux is highly anisotropic and the detector field of view, interplanetary field orientation, and planetary shadowing conspire to minimize what is measured in low Mars orbit. While the detector field of view restriction does not affect the radiation dose at the spacecraft, it can give a false impression of the frequency and/or intensity of the local SEP environment.

[22] 2. Phase changes in the SEP oscillations detected in low Mars orbit should coincide with rotations of the interplanetary magnetic field. They can in principle be used to infer the field orientation although there is a 180°

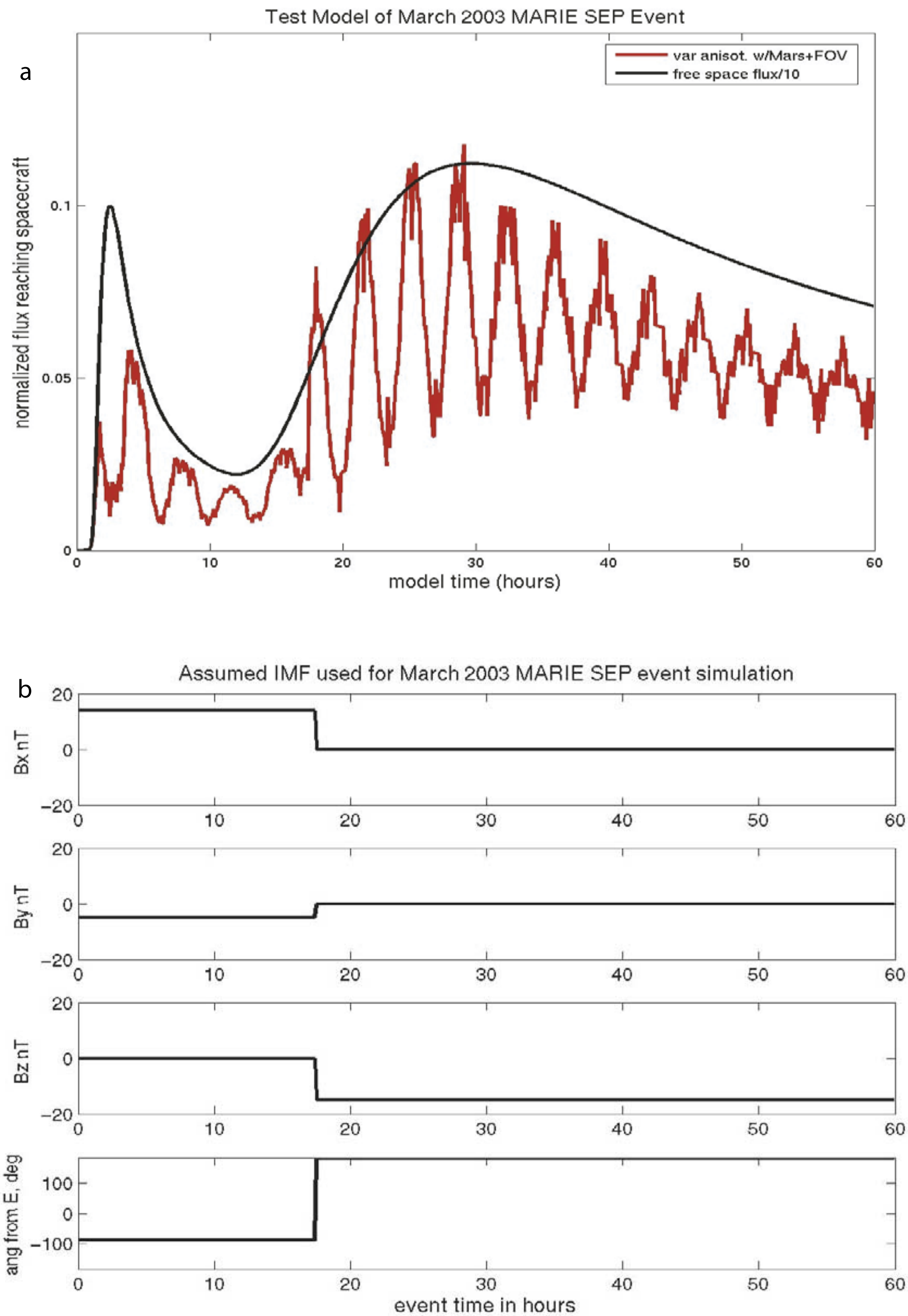

Figure 11. Figure 11a shows the model approximation to the behavior seen in the MARIE SEP event in Figure 10. This is not intended to exactly replicate the real event but to illustrate the basic idea of the potential control of the interplanetary field orientation on the phase of the oscillation produced by the geometrical considerations described in this paper. The oscillations change phase about 18 hours into the event due to the rotation of the assumed interplanetary field shown in Figure 11b. The coordinate system for the field vector components is the standard MSO system, with x pointed toward the Sun, y pointed in the direction opposite planetary motion, and z pointed north out of the plane of Mars' orbit. The addition of an x component also modifies the amplitude of the oscillations. For this model the orbital period was assumed longer than the actual one to make it easier to see the phase change.

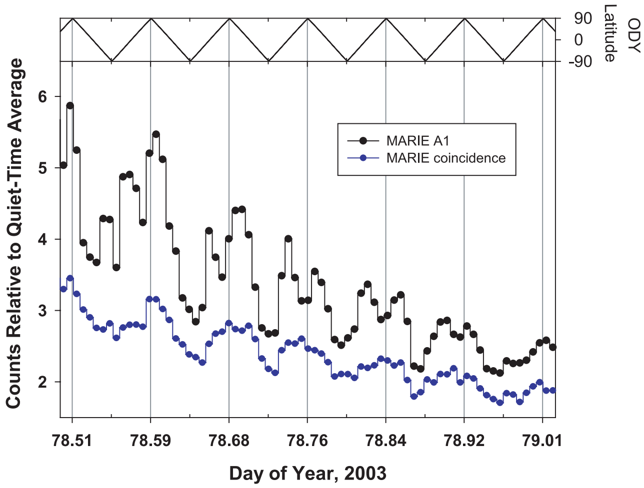

Figure 12. Details of a period of the March 2003 MARIE SEP event showing an apparent doubling of the oscillation frequency after day 77.5. This may be explained by the occurrence of counter streaming or magnetically trapped protons in the field loops of the ejected coronal material when it passes Mars.

ambiguity in direction. To the extent the SEPs permeate the interplanetary disturbance launched by a coronal mass ejection at the Sun, they can be used to diagnose the field topology. The March 2003 event flux phases follow the MGS field orientation, a result that suggests the IMF becomes highly inclined in the middle of the event. This is consistent with what is often observed when CME ejecta fields pass over an observer [e.g., *Gosling and McComas*, 1987]. Moreover, the double peaks per orbit appearing at the time of the highly inclined fields, and shown in the zoomed-in portion of the MARIE March 2003 event time series in Figure 12, may represent counterstreaming beams of solar energetic particles. These are also seen in some gradual events at the Earth [e.g., *Marsden et al.*, 1987], and are thought to indicate magnetic mirroring of the SEP ions in a magnetic bottle-like structure, or connection to a solar source of the particles at one or both ends of the passing flux tubes of the ejected coronal material. No attempt was made to introduce a bidirectional anisotropy in the calculations described here, but the modification would be straightforward.

[23] In summary, solar energetic particles in the near-Mars space environment are affected by both the presence of the planetary absorber and the varying interplanetary magnetic field orientation. Here we have shown by illustration, inspired by an event observed by the MARIE instrument on the Odyssey spacecraft, the effects of both of these factors on the detected fluxes in a low (~400 km altitude) Mars orbit. Together with the restricted field of view of the instrument, the presence of the planet diminishes the detected flux over that present in interplanetary space. A SEP field-aligned anisotropy, a frequent occurrence especially in the earlier stages of an event, produces orbital period oscillations in the fluxes that were seen by MARIE and also on the Phobos-2 spacecraft by the SLED detector. A simple model shows how the various circumstances of the particle event, the spacecraft location, and the detector field of view and orientation combine to produce a particular observed time series of particle flux with a certain depth and orbital phase dependence of the SEP flux oscillations. These considerations will affect the SEP radiation exposure of all missions in Mars orbit and on the surface, as well as their ability to interpret the local SEP event interplanetary characteristics. For example, the energetic particle telescope on MSL will see an environment where the planet is blocking nearly a hemisphere of SEP access. Although the atmosphere and surface will produce secondaries whose trajectories depart from those of the primary SEPs, interplanetary field orientation effects on total flux should still be seen during anisotropic SEP events due to geometrical exclusion of some incident primary particle trajectories.

[24] The radiation detectors planned for lunar orbit [e.g., *Chin et al.*, 2007] will also experience similar departures of SEP event behavior from the interplanetary space conditions when the Moon is upstream of the Earth's bow shock (J. Halekas, personal communication, 2005). In that case, the absence of an appreciable field signature of the lunar solar wind interaction should make the present model of the near-body SEP environment even more accurate, although the smaller lunar obstacle will affect only the most anisotropic SEP events and phases of events. In fact, much smaller gyroradius suprathermal electrons are used in lunar orbit and also at Mars for electron reflectometry experiments to probe the lunar remanent magnetic fields and the remanent field-solar wind interaction [*Halekas et al.*, 2001]. This interaction is complicated by the topological field changes that occur from remanent field reconnection with the external field. Thus any use of interplanetary electron shadowing details as a diagnostic when remanent fields are near the solar wind wake boundary must take these additional effects into account. For the SEP ions, such planetary details on the SEP shadowing are expected to be negligible, and oscillation irregularities attributable to the external SEP event details as in the example above. Nevertheless, future Mars missions preparing for human presence need to include local space measurements for comparisons with those on the surface to ensure an understanding of these and other (e.g., surface and atmosphere secondaries) important effects. The loss of the MARIE experiment has eliminated this possibility for the foreseeable future; the GRS may prove an acceptable, albeit limited, substitute.

[25] **Acknowledgments.** The authors are grateful to the previous MARIE Principal Investigator G. Badhwar (now deceased) for proposing the investigation and seeing the instrument through launch and commissioning. We are also indebted to the MGS Magnetometer PI, M. Acuña, for providing public access to that data set, which is key to the interpretation of the MARIE observations. Both data sets are archived in the Planetary Data System particles and fields node at UCLA. The UCB authors are supported for work on Mars data analysis by NASA through a subaward from SWRI (UCB award 599970Q).

References

Acuña, M. H., et al. (1999), Global distribution of crustal magnetization discovered by the Mars Global Surveyor MAG/ER experiment, *Science*, *284*, 790–793.

Boynton, W. V., et al. (2004), The Mars Odyssey Gamma-Ray Spectrometer Instrument Suite, *Space Sci. Rev.*, *110*, 37–83.

Brain, D. A., D. L. Mitchell, and J. S. Halekas (2006), The magnetic field draping direction at Mars from April 1999 through August 2004, *Icarus*, *182*, 464–473.

Cane, H. V., D. V. Reams, and T. T. von Rosenvinge (1988), The role of interplanetary shocks in the longitude distribution of solar energetic particles, *J. Geophys. Res.*, *93*, 9555–9567.

Chin, G., et al. (2007), Lunar Reconnaissance Orbiter overview: The instrument suite and mission, *Space Sci. Rev.*, *129*(4), 391–419, doi:10.1007/s11214-007-9153-y.

Cleghorn, T. F., B. S. Premkumar, C. J. Zeitlin, and F. A. Cucinotta (2004), Solar particle events observed at Mars: Dosimetry measurements and model calculations, *Adv. Space Res.*, *33*(12), 2215–2218.

Gosling, J. T., and D. J. McComas (1987), Field line draping about fast coronal mass ejecta—A source of strong out-of-ecliptic interplanetary fields, *Geophys. Res. Lett.*, *14*, 355–358.

Halekas, J. S., D. L. Mitchell, R. P. Lin, S. Frey, L. L. Hood, M. H. Acuña, and A. B. Binder (2001), Mapping of crustal magnetic anomalies on the lunar near side by the Lunar Prospector electron reflectometer, *J. Geophys. Res.*, *106*(E11), 27,841–27,852.

Kallenrode, M.-B. (1996), A statistical survey of 5-MeV proton events at transient interplanetary shocks, *J. Geophys. Res.*, *101*(A11), 24,393–24,410.

Kallio, E., J. G. Luhmann, and J. G. Lyon (1998), Magnetic field near Venus: A comparison between Pioneer Venus Orbiter magnetic field observations and an MHD simulation, *J. Geophys. Res.*, *103*(A3), 4723–4754.

Leblanc, F., J. G. Luhmann, R. E. Johnson, and E. Chassefiere (2002), Some expected impacts of a solar energetic particle event at Mars, *J. Geophys. Res.*, *107*(A5), 1058, doi:10.1029/2001JA900178.

Marsden, R. G., T. E. Sanderson, C. Tranquille, K.-P. Wenzel, and E. J. Smith (1987), ISEE-3 observations of low energy proton bidirectional events and their relation to isolated interplanetary magnetic structures, *J. Geophys. Res.*, *92*, 11,009–11,019.

McKenna-Lawlor, S., V. V. Alfonin, K. I. Gringauz, K. Keckskemety, E. Keppler, E. Kirsch, A. Richter, A. Ruznyuk, K. Schwingenschuh, and D. O'Sullivan (1992), Energetic particle studies at Mars by SLED in PHOBOS-2, *Adv. Space Res.*, *12*(9), 231–241.

McKenna-Lawlor, S. M. P., M. Dryer, C. D. Fry, W. Sun, D. Lario, C. S. Deehr, B. Sanahuja, V. A. Afonin, M. I. Verigin, and G. A. Kotova (2005), Predictions of energetic particle radiation in the close Martian environment, *J. Geophys. Res.*, *110*, A03102, doi:10.1029/2004JA010587.

Reames, D. V. (1999), Particle acceleration at the Sun and in the heliosphere, *Space Sci. Rev.*, *90*, 413–491.

Turner, R., et al. (2003), MARIE observations of solar particle events, paper presented at 14th Annual Space Radiation Health Investigators' Workshop, NASA, Houston, Tex., April.

Zeitlin, C. J., T. Cleghorn, F. Cucinotta, P. Saganti, V. Anderson, K. Lee, L. Pinsky, W. Atwell, R. Turner, and G. Badhwar (2004), Overview of the Martian radiation environment experiment, *Adv. Space Res.*, *33*(12), 2204–2210.

W. Boynton, Lunar and Planetary Laboratory, University of Arizona, 1629 E. University Boulevard, Kuiper 532, Tucson, AZ 85721, USA.

D. A. Brain, G. Delory, and J. G. Luhmann, Space Sciences Laboratory, University of California, Berkeley, Centennial Drive at Grizzly Peak Blvd., Berkeley, CA 94720, USA. (jgluhman@ssl.berkeley.edu)

J. G. Lyon, Physics and Astronomy Department, Dartmouth University, 6127 Wilder Laboratory, Hanover, NH 03755, USA.

R. Turner, ANSER, 1215 Jefferson Davis Hwy., Suite 800, Arlington, VA 22202, USA.

C. Zeitlin, Lawrence Berkeley National Laboratory, Berkeley, CA 94720, USA.